The Journal of Chemical Physics

Gold adatoms and clusters on PPV: An ab initio investigation

W. H. Brito, R. A. Silva, and R. H. Miwa

Citation: The Journal of Chemical Physics **133**, 204703 (2010); doi: 10.1063/1.3506771
View online: http://dx.doi.org/10.1063/1.3506771
View Table of Contents: http://scitation.aip.org/content/aip/journal/jcp/133/20?ver=pdfcov
Published by the AIP Publishing

Gold adatoms and clusters on PPV: An *ab initio* investigation

W. H. Brito,[1] R. A. Silva,[1,2] and R. H. Miwa[1,a)]
[1]*Instituto de Física, Universidade Federal de Uberlândia, C. P. 593, 38400-902 Uberlândia, MG, Brazil*
[2]*Divisão de Metrologia de Materiais, Instituto Nacional de Metrologia, Normalização e Qualidade Industrial, CEP: 25250-020 - Duque de Caxias - RJ, Brazil*

(Received 25 June 2010; accepted 8 October 2010; published online 30 November 2010)

We have performed an *ab initio* investigation of the energetic, structural, electronic, and vibrational properties of Au atoms and clusters adsorbed on poly-*p*-phenylene vinylene (PPV) chains, Au_n/PPV (with $n = 1, 2, 6, 7, 10$, and 12). We find that the Au_n/PPV systems are energetically stable by 0.5 eV, compared with the isolated systems, viz., PPV chain and Au_n clusters, thus supporting the formation of Au_n/PPV nanocomposites. Further support to the formation of Au_n/PPV has been provided by examining the vibrational properties of pristine PPV and Au_n/PPV systems. In agreement with experimental measurements, we find a reduction on the in-plane vibrational frequency of C–C bonds of Au_n/PPV, when compared with the same vibrational modes of pristine PPV. The electronic properties of isolated Au_n clusters are modified when adsorbed on PPV. The highest occupied states of Au_n/PPV are mostly concentrated on the Au_n cluster, while the lowest unoccupied states are mainly localized along the PPV chain. The HOMO–LUMO energy gap of the Au_n/PPV systems are smaller than the energy gap of the isolated systems, Au_n clusters, and pristime PPV chains. © *2010 American Institute of Physics*. [doi:10.1063/1.3506771]

I. INTRODUCTION

Organic conjugated polymers have been considered as promising materials to build up new electronic and optoelectronic devices.[1] In particular, poly-*p*-phenylene vinylene (PPV) conjugated polymers have been the subject of numerous studies addressing their electronic, structural, and vibrational properties. PPV exhibits a semiconducting character, with an energy band gap of 2.4 eV (exp.).[2,3] We may increase the applicability of PPV by adding other chemical elements or by adding side chains in its conjugated segment. Indeed, very recently freestanding thin conjugated films (width below 20 nm) of poly(2,5-methoxypropyloxy sulfonate phenylene vinylene), MPS-PPV, has been successfully synthesized, providing suitable mechanical properties to fabricate large luminescent panels.[4] The atomic structure of PPV monomers is quite similar to the one of stilbene molecules. X-ray diffraction results on stilbene molecular crystals[5] have been used as a reference in several *ab initio* theoretical investigations on the equilibrium geometry of PPV.[6,7] Further theoretical studies have been performed focusing on the electronic,[8,9] transport,[10] and vibrational properties[6,11–13] of pristine PPV.

The interaction of PPV molecules with foreign atoms and molecules is an important issue to be investigated. In many cases, the presence of those foreign elements is somewhat unintentional, for instance, at the metal/polymer interface we may find metallic elements incorporated into the polymer layers. In particular, for Al cathodes in contact with PPV, experimental works verified that the Al atoms are incorporated by $\sim$30 Å into PPV films.[14] Theoretical calculations have been performed addressing the initial stage of the formation of metal/PPV interfaces[15] and the doping processes with metallic elements (Ca, Mg, and Al).[16] Based upon x-ray and ultraviolet photoelectron spectroscopy (XPS and UPS) experiments, Au/PPV interfaces have been investigated.[17] Similar to the Al/PPV interface, the incorporation of Au into the PPV oligomer films is observed. In contrast to the unintentional presence of metallic structures, very recently metallic nanoclusters have been intentionally embedded into organic polymers.[18–20] In those systems, the organic films may play a role of mechanical support to the inorganic nanoparticles, giving rise to self-organized structures, like superlattices of quantum dots. On the other hand, the electronic properties of the nanoparticles can be tuned in a suitable way through electronic interactions between the nanoparticle and the organic film, for instance, in CdSe/ZnS quantum dots adsorbed in polymer films[21] and in the very recently synthesized poly[2-methoxy, 5-(2-ethylhexoxy)-1,4-phenylene vinylene] (MEH-PPV)/gold nanoparticles.[22] In the latter system, experimental works indicate that the photoluminescence of MEH-PPV/Au nanoparticle increases when compared with the photoluminescence intensity of pristine Au nanoparticles.

In this paper we present a detailed investigation on Au atoms and clusters adsorbed onto PPV chains, Au_n/PPV. We perform an *ab initio* investigation of the structural, energetic, electronic, and vibrational properties of Au_n/PPV (for $n = 1$, 2, 6, 7, 10, and 12). The calculation approach is described in Sec. II. Initially we studied the pristine systems, viz., isolated PPV chains and Au_n clusters, in order to verify the adequacy of our calculation procedure (Sec. III A) and then we start to investigate the Au_n/PPV system (Sec. III B). For each Au_n/PPV structure, the energetically more stable configuration has been determined, and the electronic and vibrational properties have been examined. In Sec. IV we present a summary of our results.

[a)]Author to whom correspondence should be addressed. Electronic mail: hiroki@infis.ufu.br.

II. METHOD OF CALCULATION

Our calculations were performed within the density functional theory (DFT),[23] using the spin-polarized Perdew–Burke–Ernzerhof generalized gradient approximation (PBE–GGA) scheme to calculate the electron–electron interactions.[24] In the present investigation we have used two different calculation approaches. (i) For the structural, energetic, and electronic properties, the Au_n/PPV system was described within the supercell approach, where we have considered a PPV chain composed by four PPV monomers in an orthorhombic supercell with $a = 13.5$ Å, $b = 27$ Å, and $c = 26.976$ Å. The respective Brillouin zone sampling was performed using a set of nine special k-points.[25] The lattice parameter c, parallel to the PPV chain, was minimized with respect to the total energy. The electron–ion interaction was described by using norm-conserving pseudopotentials,[26] and the Kohn–Sham wave functions[27] were expanded in a linear combination of numerical pseudoatomic orbitals, using a split-valence double-zeta basis set and including polarization functions.[28] Since pseudoatomic orbitals are computationally more efficient to describe larger systems, mainly when we have large vacuum regions within our supercell. Those calculations were performed using the SIESTA code.[29] The atomic relaxations were performed by using the conjugated gradient scheme, within a force convergence of 0.05 eV/Å. (ii) The calculation of the vibrational properties was performed within the density functional perturbation theory (DFPT) approach,[30] as implemented in the PWSCF code,[31] in order to include the polarizability effects on the vibrational modes and frequencies. The electron–ion interactions were described using ultrasoft pseudopotentials,[32] and PBE-GGA approach to the electron–electron exchange-correlation. In this case, the Kohn–Sham wave functions were expanded in a plane-wave (charge density) basis set, with an energy cutoff of 30 Ry, expanded to 120 Ry for charge density calculation.[33] The supercell size was reduced to $a = b = 20$ Å and $c = 6.744$ Å, and we have considered 54 special k-points to the Brillouin zone sampling.[13,34] For the atomic relaxations, the force convergence criterion was reduced to 0.005 eV/Å.

III. RESULTS AND DISCUSSIONS

A. Pristine PPV and Au_n clusters

Initially we examined the structural, electronic, and vibrational properties of pristine systems, viz., PPV and Au_n clusters. Figure 1 presents the structural model and the total charge density along the PPV chain. At the equilibrium geometry the C–C and C–H bond lengths, summarized in Table I, are slightly larger compared with previous theoretical calculations,[6,7] being in accordance with the different choice for the exchange-correlation functionals. However, we find the same picture for the C–C and C–H bond lengths along the PPV chain, namely (i) the 7–8 (double) bond in the vinylene is compressed compared with the other C–C bonds, while (ii) the C–H bond lengths are practically the same along the PPV chain. X-ray diffraction measurements, for the herringbone crystal phase of PPV, indicate a lattice constant (c for a monoclinic unit cell) of 6.54 Å. Here we find a monomer length (1a–1b in Table I) of 6.74 Å for insolated PPV chains, while in Refs. 6 and 7 the authors obtained 6.65 Å using the local density approximation (LDA) to describe the exchange-correlation term. The PPV chain exhibits a semiconducting character, with an energy band gap of 1.2 eV (theor.) calculated within the DFT approach. Our calculated HOMO and LUMO (partial) charge density distributions compare very well with the ones presented in Refs. 7 and 10. There is no contribution from C–H bonds to the HOMO (LUMO), since the C–H states are localized at 3.6 eV (4.5 eV) below (above) the valence band maximum (conduction band minimum).

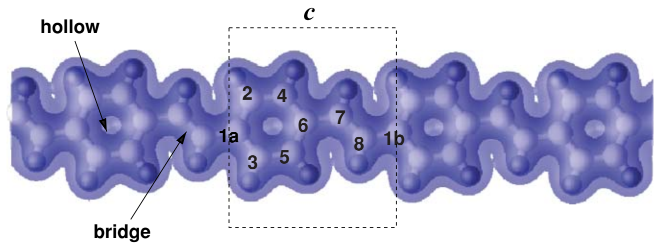

FIG. 1. Structural model and the total charge density of an isolated PPV chain. The isosurfaces correspond to total charge densities of 0.01 and 0.05 e/bohr^3.

We next examine the vibrational normal-modes of the pristine PPV chain. We find that the in-plane (ip) modes coming from C–C ring, within the frequency range of 1297.9–1534.7 cm^{-1}, and the vinylene C–C stretch mode of 1609.2 cm^{-1} are in good agreement with experimental Raman and infrared[35–38] results, as well as *ab initio* total energy calculations.[6,13] Our vibrational frequencies, calculated at the Γ point, are summarized in Table II. We have done similar DFPT calculations as performed by Zheng *et al.*;[13] however, we made a different choice for the exchange correlation energy. That is, we used the PBE-GGA approach, while Zheng *et al.* considered the LDA.[39] The vibrational frequencies from the C–H modes are higher than 3000 cm^{-1}.

The calculated equilibrium geometries of Au clusters, Au_n (with $n = 2$, 6, 7, 10, and 12), are depicted in Fig. 2. Here we have considered a large tetragonal supercell (27×13 ×27 Å) in order to avoid the interaction between an Au_n cluster and its (periodic) image. For those clusters we calculate the binding energy by comparing the total energies of Au_n and n

TABLE I. C–C and C–H equilibrium bond lengths (in angstrom) for an isolated PPV chain.

Atoms	This work	Ref. 6	Ref. 7
1a–1b	6.747	6.65	6.65
1a–2	1.428	1.411	1.401
2–4	1.401	1.383	1.375
1a–3	1.430	1.414	1.403
6–7	1.463	1.443	1.451
7–8	1.377	1.361	1.349
2–H	1.110	1.103	1.096
3–H	1.112	1.104	1.096
7–H	1.113	1.108	1.101

TABLE II. Our calculated frequencies of the normal vibrational modes at the Γ point (in cm^{-1}). The modes are described as in-plane (ip) and out-of-plane (op). The calculations were performed using a plane wave basis set (see details in Sec. II).

Symmetry	Description	This work	Ref. 13	Ref. 6
B_g	op	138.0	121.7	147
A_u	op	236.2	220.9	220
A_g	ip	307.5	323.9	310
B_g	op	311.6	324.6	327
A_u	op	404.4	406.2	390
B_u	ip	416.8	432.6	430
A_u	op	547.9	553.3	532
A_g	ip	623.9	639.7	622
A_g	ip	651.4	672.6	659
B_g	op	700.1	720.9	696
B_g	op	776.6	794.9	785
B_u	op	802.1	810.6	799
A_u	op	831.3	841.2	818
B_g	op	851.8	882.4	853
A_g	ip	873.7	893.7	899
A_u	op	934.6	957.2	911
B_g	op	942.8	963.0	926
A_u	op	960.2	968.2	930
B_u	ip	993.9	1011.2	978
B_u	ip	1093.2	1113.4	1076
A_g	ip	1136.5	1151.3	1111
A_g	ip	1183.0	1208.4	1185
B_u	ip	1200.6	1224.7	1187
A_g	ip	1267.6	1294.3	1262
B_u	ip	1279.7	1296.9	1268
A_g	ip	1297.9	1314.1	1274
B_u	ip	1352.1	1376.0	1367
B_u	ip	1411.9	1442.2	1458
B_u	ip	1495.4	1505.7	1485
A_g	ip	1495.7	1523.7	1493
A_g	ip	1534.7	1553.1	1546
A_g	ip	1609.2	1637.4	1635
A_g	ip	3032.1	3038.9	2951
B_u	ip	3043.0	3051.3	2975
A_g	ip	3059.1	3074.1	3058
B_u	ip	3064.0	3078	3064
A_g	ip	3083.9	3101.2	3116
B_u	ip	3089.1	3102.9	3125.1

isolated Au atoms. As indicated in Table III, our results of binding energies are smaller by ∼10% when compared with the ones obtained by Fernández *et al.*[40] However, the relative stability has been maintained, namely, Au_{12} represents the energetically more stable structure, followed by Au_{10}, while Au_7 is the energetically less favorable structure.

B. Au_n clusters adsorbed on PPV chains

Once the electronic, structural, vibrational, and energetic properties of the pristine systems have been successfully described, in agreement with previous results, we next start the investigation of Au (atomic and cluster) adsorption on the PPV chains. For a single Au adatom on the PPV chain, Au_1/PPV, we have considered the adsorption sites indicated in Fig. 1. Our calculated adsorption energies indicate that the

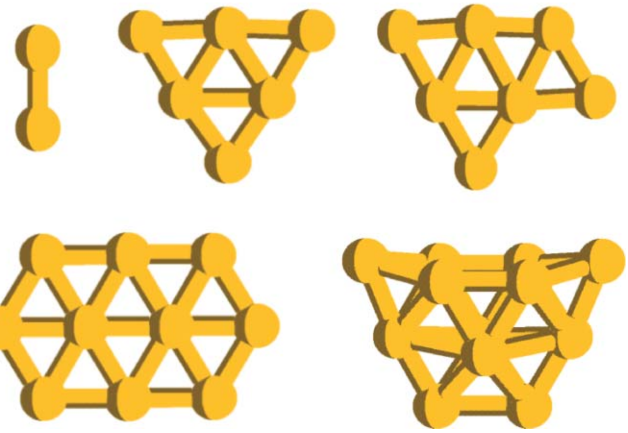

FIG. 2. Structural models of the Au_n clusters for $n = 2$, 6, 7 10, and 12. The calculated binding energies are presented in Table III.

Au adatom lying on top of the vinyl carbon atom (sites 7 or 8) is more likely when compared with the Au adsorption on the phenyl carbon atoms. Au adatoms on top of the C atoms of the phenyl ring are energetically less stable by 0.22–0.32 eV. In contrast, we find that the Au adsorption on the PPV hollow or bridge sites is quite unlikely, since (in both cases) the Au adatom segregates toward the top sites of the carbon atoms. At the equilibrium geometry, for Au adatom on the vinyl C atom, the C(7)–Au bond length, 2.15 Å, is very close to the sum of the Au and C covalent radii, 1.43 and 0.77 Å, respectively, suggesting the formation of C–Au chemical bond. In addition, due to the fourfold coordination of vinyl carbon atom bonded to Au, the double-bond character along C(7)–C(8) has been suppressed, and the C(7)–C(8) bond length increases by 0.064 Å (1.377→1.441 Å).

Figure 3(a) presents the projected density of states (PDOS) of pristine PPV (shaded region) and Au_1/PPV (solid line) systems. We find that the electronic states of PPV are perturbed, due to the Au adsorption, within an energy interval up to 7 eV below the Fermi level. The occupied electronic states of Au adatoms, dashed lines in Fig. 3(a), are mostly localized within an energy interval of 4 eV below the Fermi level. Where the Au 5d states are concentrated within an energy interval between −3 and −1.5 eV, while the Au 6s orbitals are mainly localized within the fundamental band gap. There is an energy splitting of ∼0.55 eV between a spin-up (occupied) and spin-down (unoccupied) states, composed by Au 6s and C(8) 2p orbitals (carbon atom nearest neighbor to the C–Au bond) [Fig. 3(b)]. In addition, in the same diagram [Fig. 3(b)] we verify that there is a reduction on the highest occupied and the lowest unoccupied

TABLE III. Our calculated binding energy of Au_n clusters (in eV/atom).

Au_n	This work	Ref. 40
2	1.30	1.5
6	2.27	2.56
7	2.24	2.52
10	2.48	2.72
12	2.57	2.87

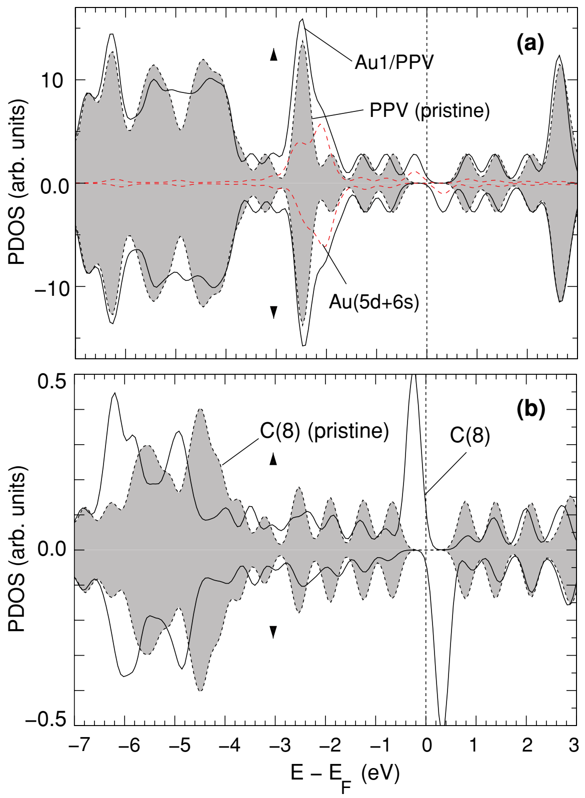

FIG. 3. (a) Projected density of states (PDOS) of the energetically more stable Au_1/PPV system. Solid (dashed) lines represent the PDOS of the Au_1/PPV (adsorbed Au 5d and 6s orbitals), and the shaded regions indicate the PDOS of the pristine PPV. (b) PDOS of the vinyl carbon atom nearest neighbor to the C(7)–Au bond, C(8).

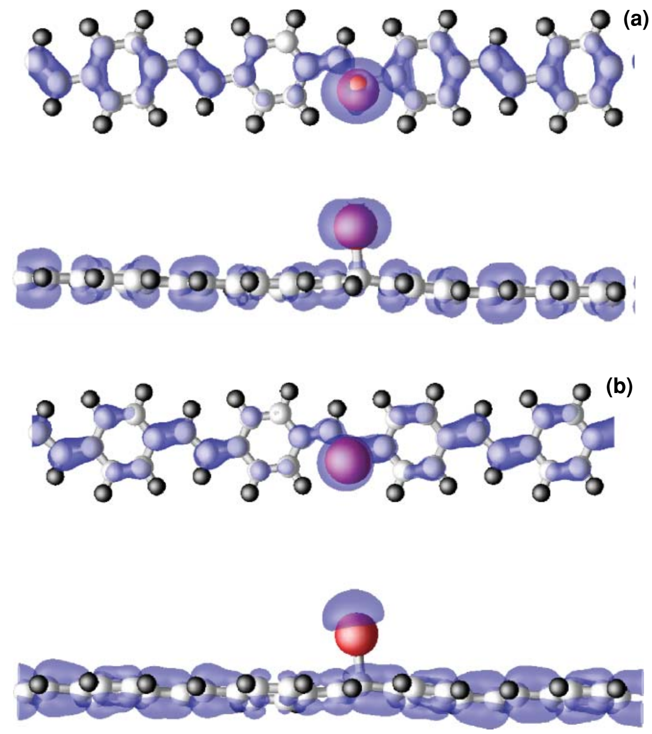

FIG. 4. Top-view and side-view of the HOMO (a) and LUMO states (b). The isosurfaces correspond to charge densities of $2\times10^{-4} e/\text{bohr}^3$.

electronic density of states, which is in accordance with the (local) reduction of HOMO and LUMO nearby the C–Au bond [Figs. 4(a) and 4(b), respectively].

The energetic stability of Au_n/PPV can be inferred by calculating the binding energy of Au_n clusters adsorbed on PPV chains (E_n^b). E_n^b can be written as

$$E_n^b = E[\text{PPV}] + E[\text{Au}_n] - E[\text{Au}_n/\text{PPV}] + \delta^{\text{BSSE}},$$

where E[PPV] and $E[\text{Au}_n]$ represent the total energies of the isolated systems, PPV chains and Au_n clusters, respectively, and $E[\text{Au}_n/\text{PPV}]$ represents the total energy of the Au_n/PPV system. The last term, δ^{BSSE}, has been included to correct the so-called basis set superposition errors (BSSE).[41] This is due to the use of atomic orbitals, to expand the KS wave functions, in the present calculation approach (see Sec. II). Here, δ^{BSSE} was calculated following the procedure proposed in Refs. 42 and 43. In particular, for a single adatom adsorbed on PPV we examined the adequacy of our calculation procedure for E_n^b by increasing the orbital size, i.e., the cutoff radius of the atomic orbitals. Within the SIESTA code, the cutoff radius of the basis set (atomic orbitals) can be tuned by a single parameter, *energy shift*.[29] For lower *energy shift* we have larger cutoff radii for the atomic orbitals, that is, the basis set has been improved. For an *energy shift* of 0.1 eV (0.05 and 0.025 eV) we find E_1^b of 0.56 eV (0.51 and 0.50 eV, respectively). Thus, indicating that an *energy shift* of 0.1 eV is suitable enough to describe the Au_n/PPV systems. Recent *ab initio* calculations of Au on graphene indicate similar results for binding energy and equilibrium geometry, for instance, binding energies between 0.3 and 0.8 eV and C–Au bond length of 2.25–2.44 Å on top of the carbon atom.[44,45]

We next examined the total energies of a number of plausible configurations for Au_n clusters adsorbed on the PPV chain. Table IV presents the calculated binding energies (for the energetically most stable configurations) of Au_n/PPV, for $n = 1$, 2, 6, 7, 10, and 12. It is worth noting that the high binding energy for Au_2 dimer adsorbed on PPV is due to the lower cohesive energy of isolated Au_2 dimers (1.5 eV) when compared with the other Au_n clusters (2.3 – 2.6 eV for $n=6$ – 12) (see Table III). The binding energies Au_6 and Au_7 isolated clusters are very close (2.27 and 2.24 eV, respectively), while our calculated adsorption energies indicate that Au_7/PPV is slightly more stable than Au_6/PPV. Similar to the Au adatoms and dimers on PPV, there is an energetic preference for Au_6 and Au_7 clusters adsorbed on the vinyl C atoms. The Au_6 and Au_7 clusters adsorb on the bridge site between C(7) and C(8), giving rise to two C–Au bonds. At the

TABLE IV. Our calculated binding energies (E^b) for the most likely configurations of Au_n/PPV.

Au_n/PPV	E_n^b (eV)
Au_1/PPV	0.56
Au_2/PPV	1.01
Au_6/PPV	0.47
Au_7/PPV	0.56
Au_{10}/PPV	0.54
Au_{12}/PPV	0.47

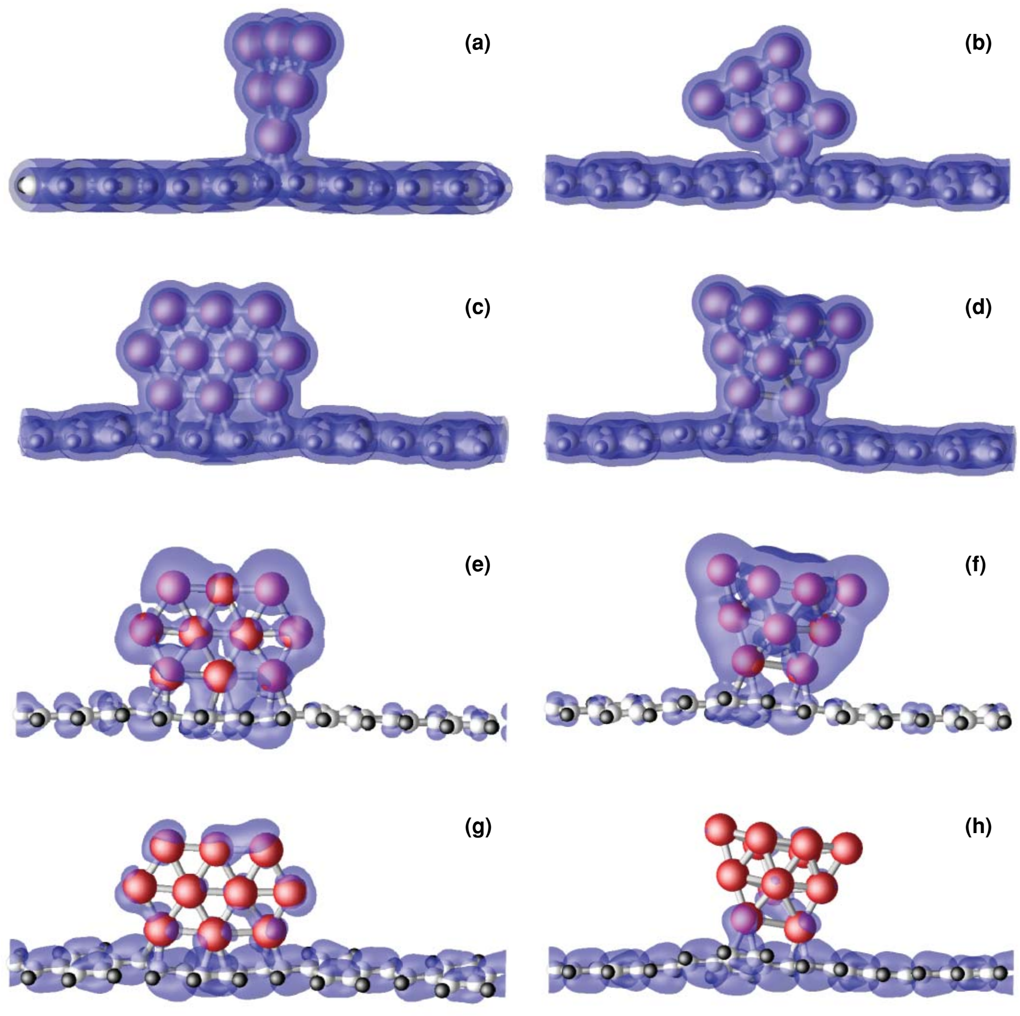

FIG. 5. Side-view of the total charge densities of Au_6/PPV (a), Au_7/PPV (b), Au_{10}/PPV (c), and Au_{12}/PPV (d) systems. The isosurfaces correspond to total charge densities of 0.01 and 0.05 e/bohr^3. Partial charge densities of HOMO of Au_{10}/PPV (e) and Au_{12}/PPV (f), and LUMO of the Au_{10}/PPV (g) and Au_{12}/PPV (h) structures. The isosurfaces of HOMO and LUMO correspond to charge densities of 3 and 5×10^{-4} e/bohr^3, respectively.

equilibrium geometry, the C–Au bond lengths are 2.32 and 2.28 Å, for Au_6/PPV and Au_7/PPV systems, respectively, and the C(7)–C(8) bond length increases to 1.42 Å. In both systems, Au_6/PPV and Au_7/PPV, there is just a single Au atom of the cluster attached to the PPV chain. However, the shorter C–Au bonds in Au_7/PPV indicate that their covalent character has been strengthened in comparison with the ones in Au_6/PPV, thus, in consonance with the higher binding energy obtained for Au_7/PPV. Figures 5(a) and 5(b) present the equilibrium geometry and the total charge densities of Au_6/PPV and Au_7/PPV, respectively, indicating the formation of C–Au chemical bonds. Focusing on the electronic properties, we find that the occupied electronic states of Au_6 and Au_7 adsorbed on PPV are mostly localized at ~4 eV below the valence band maximum. In addition, similar to Au_1/PPV, in the Au_7/PPV structure we find unpaired electronic states within the fundamental band gap, attributed to Au 6s and 2p orbitals of the vinyl C atom neighbor to the C–Au bond.

Even for larger and energetically more stable Au_n clusters (Au_{10} and Au_{12}), our calculated binding energies indicate that the formation of Au_{10}/PPV and Au_{12}/PPV structures are exothermic processes. Figures 5(c) and 5(d) present the total charge densities of the Au_{10}/PPV and Au_{12}/PPV systems, respectively. Different from the Au_6/PPV and Au_7/PPV systems, we find C–Au chemical bonds on the vinyl as well on the phenyl carbons atoms along the PPV chain. At the equilibrium geometry we have C–Au bond lengths between 2.25 and 2.55 Å, and the Au clusters are slightly distorted when compared with the isolated structures. Here, we can infer that the binding energies of Au_{10}/PPV and Au_{12}/PPV are ruled by the number of Au atoms of the cluster attached to the PPV chain. That is, in Au_{10}/PPV we have three C–Au bonds ($E^{\mathrm{b}}_{10} = 0.54$ eV), while in Au_{12}/PPV we find two C–Au bonds ($E^{\mathrm{b}}_{12} = 0.47$ eV). In addition, similar to the other Au_n/PPV systems, the C(7)–C(8) bond length increases to 1.42 Å, suggesting that the double bond character of PPV has been suppressed upon Au_n adsorption. This is in accordance with the XPS and UPS experimental results for Au/PPV interfaces.[17]

Focusing on the electronic properties, we find that Au_{10}/PPV and Au_{12}/PPV present semiconducting characters, with the HOMO–LUMO energy gaps of 0.67 and 0.69 eV,

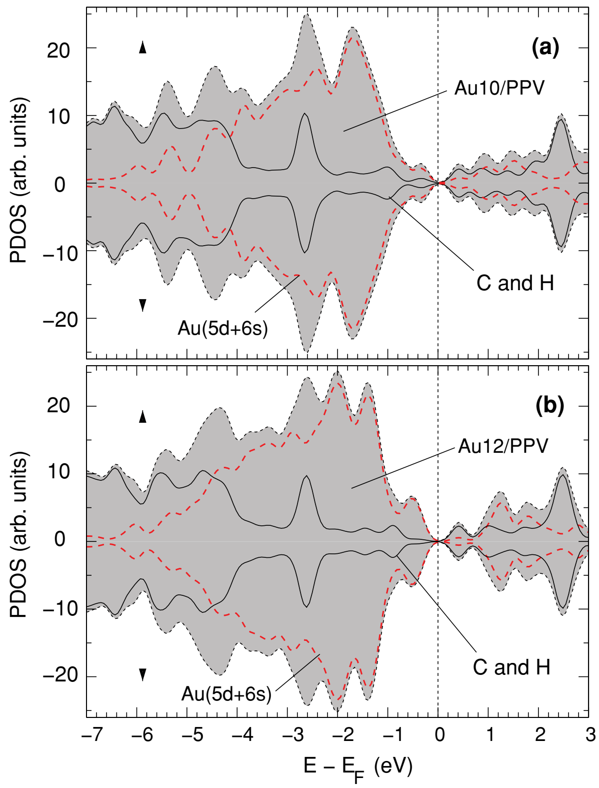

FIG. 6. Projected density of states (PDOS) of the Au_{10}/PPV (a) and Au_{12}/PPV (b) systems (shaded regions). Solid (black) lines represent the PDOS of the C and H atoms, and the dashed (red) lines represent the PDOS of Au 5d and 6s orbitals of the adsorbed clusters.

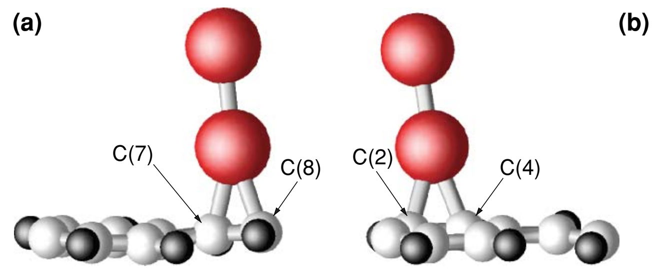

FIG. 7. Structural models of Au_2 dimers on PPV. (a) Au_2 on the vinyl C(7)–C(8) atoms and (b) Au_2 on the phenyl C(2)–C(4) atoms.

respectively, calculated within the DFT approach. There is an energy gap reduction when compared with the isolated systems, namely, Au_{10} (1.32 eV), Au_{12} (0.97 eV), and pristine PPV (1.20 eV). Figures 6(a) and 6(b) present the PDOS of the Au_{10}/PPV and Au_{12}/PPV systems, respectively. In those diagrams the shaded regions represent the total density of states. For both systems, we find that the valence band maximum is mainly composed by Au 5d and 6s orbitals [dashed (red) lines in Fig. 6]. Whereas the conduction band minimum is ruled by C 2p orbitals [solid (black) lines]. There is a charge separation between HOMO and LUMO. Indeed this is what we observe on the partial charge densities depicted in Figs. 5(e)–5(h). There is a strong contribution from Au clusters on the HOMO orbitals, while the LUMO orbitals spread out along the C chains of PPV.

In order to get a (general) picture of the changes on the vibrational properties of PPV due to the formation of C–Au bonds, we examine the vibrational properties of Au_2 dimers adsorbed on a PPV chain (Fig. 7). Those systems somewhat mimic the C–Au and C–C bonds of the Au_n/PPV structures depicted in Fig. 5. That is, (i) the Au_2 dimers are adsorbed on the bridge sites of C–C bonds of vinyl [Fig. 7(a)] and phenyl [Fig. 7(b)] carbon atoms, forming two C–Au bonds similarly to the other Au_n/PPV systems, (ii) the C–Au and the (bridge) C–C equilibrium bond lengths, ~2.3 and 1.4 Å, respectively, are comparable to the ones obtained for the larger Au_n/PPV systems, and (iii) the electronic hybridization of Au adatom in Au_2/PPV, $5d^{9.5}$ $6s^{1.1}$, due to the formation of C–Au bond is similar to the ones obtained to the other Au_n/PPV structures. Thus, we believe that the changes on the vibrational properties of Au_n/PPV structures will be comparable to those obtained for the Au_2/PPV system. However, it is worth pointing out that within this Au_2 dimer on PPV approach, we cannot examine the effects on the vibrational properties due to the distortion of the PPV chains verified for larger Au_{10}/PPV and Au_{12}/PPV systems. Pristine PPV chain exhibits a C_{2h} symmetry, which reduces to C_2 and C_1 due to the presence of Au_2 on the bridge site along the C(7)–C(8) and C(2)–C(4) bonds, respectively. Upon the formation of C(7)–Au and C(8)–Au bonds [Fig. 7(a)], the C(7)–C(8) and C(2)–C(4) ip stretch modes with frequency of 1609.2 cm^{-1} (for the pristine system) are shifted to 1582.1 cm^{-1} (1609.2→1582.1 cm^{-1}), where the contribution from C(7)–C(8) stretch mode is mostly suppressed. In addition, the vibrational frequency of 311.6 cm^{-1}, C(7)–C(8) out-of-plane (op) bend mode, changes to 463 cm^{-1}. In this case, we find a strong contribution from the C–Au stretch modes. The C–H ring ip bend and C(7)–C(8) stretch modes at 1495.7 cm^{-1} reduce to 1474.5 cm^{-1} due to the formation of C(2)–Au and C(4)–Au bonds [Fig. 7(b)]. While the op bend mode of the phenyl C atoms at 404.3 cm^{-1}, for the pristine PPV, goes to 414.5 cm^{-1}, the ip stretch modes of C(2)–C(4) and C(6)–C(7), both parallel to the PPV chain, reduce by ~10 cm^{-1}, 1182.9→1171.4 cm^{-1}. We check the accuracy of those results with respect to the size of the basis set.[33]

Finally, we compare our calculated vibrational properties with the ones obtained through Raman spectroscopy measurements on thin Au films deposited onto PPV (Au_{film}/PPV). Details on the growth process and optical characterizations of Au_{film}/PPV can be found elsewhere.[46] The experimental results indicate that the ip bend mode, atoms C(1a) and C(6) of the phenyl ring, reduces by ~10 cm^{-1} upon Au deposition onto PPV, viz., 1089.7→1080 cm^{-1}. Meanwhile within our theoretical approach, we find a frequency of 1093.2 cm^{-1} for the same mode for the pristine PPV, which reduces to 1073.0 cm^{-1} for Au_2 sitting on the phenyl ring [Fig. 7(b)]. Whereas for Au_2 on the vinyl atoms [Fig. 7(a)], there is an increase of 7 cm^{-1} for the same mode, namely, 1093.2→1100.1 cm^{-1}. We can infer an overall reduction on the vibrational frequency of ~13 cm^{-1} for this mode, which is in good agreement with the experimental result. Those results support the adequacy of our calculation procedure for the vibrational properties of the Au_n/PPV systems, and thus provide additional support to the adsorption process of Au_n clusters on PPV chains.

IV. SUMMARY

We have performed an *ab initio* total energy investigation of the adsorption process of Au atoms and clusters on PPV chains. We find that the formation of Au_n/PPV structures (for $n = 1$, 2, 6, 7, 10, and 12) is an exothermic process, with the formation of C–Au chemical bonds, and binding energies of around 0.5 eV, thus supporting the formation of Au_n/PPV systems. At the equilibrium geometry we obtained C–Au bond lengths between 2.2 and 2.5 Å. For single Au adatom and small Au_n clusters adsorbed on PPV, we find that there is an energetic preference for the formation of C–Au chemical bonds with the vinyl carbons atoms, C(7) and C(8) [Fig. 1]. Whereas for larger Au_n clusters, $n = 10$ and 12, we find C–Au chemical bonds with both vinyl and phenyl carbon atoms. The highest occupied states of Au_n/PPV systems become mostly composed by Au 5d and 6s orbitals, while the lowest unoccupied states are mainly localized on the C atoms along the PPV chain. The HOMO–LUMO energy gap of the Au_n/PPV system is reduced when compared with the ones of the isolated systems. These results indicate that the electronic properties of Au_n clusters will be modified in Au_n/PPV nanocomposites. Vibrational properties have been examined and compared with the experimental measurements. Here we obtained further confirmation of the formation of energetically stable Au_n/PPV. We find that (in general) there is a frequency reduction of around 10 cm^{-1} for the C–C ip stretch and bend modes nearby the Au adsorption sites. We compare our calculated results with the experimental findings for the ip bend mode of C(1a) and C(6) atoms, 1089.7 cm^{-1} (exp.), where we find a very good agreement between the theory and the experiment.

ACKNOWLEDGMENTS

The authors acknowledge financial support from the Brazilian agencies CNPq and FAPEMIG, and the computational support from CENAPAD/SP.

[1] R. H. Friend, R. W. Gymer, A. B. Holmes, J. H. Burroughes, R. N. Marks, C. Taliani, D. D. C. Bradley, D. A. D. Santos, J. L. Brédas, M. Lögdlund *et al.*, Nature **397**, 121 (1999).
[2] K. F. Voss, C. M. Foster, L. Smilowitz, D. Mihailović, S. Askari, G. Srdanov, Z. Ni, S. Shi, A. J. Heeger, and F. Wudl, Phys. Rev. B **43**, 5109 (1991).
[3] A. Marletta, R. H. Miwa, T. Cazati, F. E. G. Guimarães, R. M. Faria, and M. Veríssimo-Álves, Appl. Phys. Lett. **86**, 141907 (2005).
[4] Y. Lin, C. Jiang, J. Xu, Z. Lin, and V. V. Tsukruk, Soft Matter **3**, 432 (2007).
[5] C. J. Finder, M. G.Newton, and N. L. Allinger, Acta Cryst. B **30**, 411 (1974).
[6] R. B. Capaz and M. J.Caldas, Phys. Rev. B **67**, 205205 (2003).
[7] G. Zheng, S. J. Clark, S. Brand, and R. A. Abram, J. Phys.: Condens. Matter **16**, 8609 (2004).
[8] P. G. Costa, R. G. Dandrea, and E. M. Conwell, Phys. Rev. B **47**, 1800 (1993).
[9] A. Ferreti, A. Ruini, E. Molinari, and M. J. Caldas, Phys. Rev. Lett. **90**, 086401 (2003).
[10] A. Ferreti, A. Ruini, G. Bussi, E. Molinari, and M. J. Caldas, Phys. Rev. B **69**, 205205 (2004).
[11] D. Raković, R. Kostić, L. A. Gribov, and I. E. Davidova, Phys. Rev. B **41**, 10744 (1990).
[12] T. Hrenar, R. Mitrić, Z. Meić, H. Meier, and U. Stalmach, J. Mol. Struct. **661–662**, 33 (2003).
[13] G. Zheng, S. J. Clark, P. R. Tulip, S. Brand, and R. A. Abram, J. Chem. Phys. **123**, 024904 (2005).
[14] M. Fahlman and W. R. Salaneck, Surf. Sci. **500**, 904 (2002).
[15] V. E. Choong, Y. Park, B. R. Hsieh, and Y. Gao, J. Phys. D: Appl. Phys. **30**, 1421 (1997).
[16] A. Mabrouk, K. Alimi, P. Moliné, and T. P. Nguyen, J. Phys. Chem. B **110**, 1141 (2006).
[17] V. Papaefthimiou, A. Siokou, and S. Kennou, Surf. Sci. **532-535**, 255 (2003).
[18] C. Jiang, S. Markutsya, Y. Pikus, and V. V. Tsukruk, Nat. Mater. **3**, 721 (2004).
[19] K. Mueggenburg, X.-M. Lin, R. H. Goldsmith, and H. M. Jaeger, Nat. Mater. **6**, 656 (2006).
[20] C. Jiang, S. Singamaneni, E. Merrick, and V. V. Tsukruk, Nano Lett. **6**, 2254 (2006).
[21] D. Zimnitsky, C. Jiang, J. Xu, Z. Lin, and V. V. Tsukruk, Langmuir **23**, 4509 (2007).
[22] M. S. Kim, D. H. Park, E. H. Cho, K. H. Kim, Q.-H. Park, H. Song, D.-C. Kim, J. Kim, and J. Joo, ACS Nano **3**, 1329 (2009).
[23] P. Hohenberg and W. Kohn, Phys. Rev. **136**, B864 (1964).
[24] J. P. Perdew, K. Burke, and M. Ernzerhof, Phys. Rev. Lett. **77**, 3865 (1996).
[25] H. J. Monkhorst and J. D. Pack, Phys. Rev. B **13**, 5188 (1976).
[26] N. Troullier and J. L. Martins, Phys. Rev. B **43**, 1993 (1991).
[27] W. Kohn and L. J. Sham, Phys. Rev. **140**, A1133 (1965).
[28] E. Artacho, D. Sánchez-Portal, P. Ordejón, A. Garcia, and J. M. Soler, Phys. Status Solidi B **215**, 809 (1999).
[29] J. M. Soler, E. Artacho, J. D. Gale, A. García, J. Junquera, P. Ordejón, and D. Sánchez-Portal, J. Phys.: Condens. Matter **14**, 2745 (2002).
[30] S. Baroni, S. de Gironcoli, A. D. Corso, and P. Giannozzi, Rev. Mod. Phys. **73**, 515 (2001).
[31] P. Giannozzi *et al.*, J. Phys.: Condens. Matter **21**, 395502 (2009).
[32] D. Vanderbilt, Phys. Rev. B **41**, 7892 (1990).
[33] We verify the convergence of our vibrational frequency results with respect to the energy cutoff for the charge density calculations. By increasing the cutoff to 240 Ry, i.e., 120→240 Ry, we find differences smaller than 4% on the calculated vibrational frequencies.
[34] M. Lazzeri and F. Mauri, Phys. Rev. Lett. **90**, 036401 (2003).
[35] M. Baïtoul, J. Wery, J. P. Buisson, G. Arbuckle, H. Shah, S. Lefrant, and M. Hamdoume, Polymer **41**, 6955 (2000).
[36] I. Orion, J. P. Buisson, and S. Lefrant, Phys. Rev. B **57**, 7050 (1998).
[37] A. Sakamoto, Y. Furukawa, and M. Tatsumi, J. Phys. Chem. **96**, 1490 (1992).
[38] B. Tian, G. Zerbi, and K. Müllen, J. Chem. Phys. **95**, 3198 (1991).
[39] D. M. Ceperley and B. J. Alder, Phys. Rev. Lett. **45**, 566 (1980).
[40] E. Fernández, J. Soler, I. L. Garzón, and L. C. Balbás, Phys. Rev. B **70**, 165403 (2004).
[41] S. F. Boys and F. Bernardi, Mol. Phys. **19**, 553 (1970).
[42] J. A. Sordo, THEOCHEM **537**, 245 (2001).
[43] C. Hobbs, K. Kantorovich, and J. D. Gale, Surf. Sci. **591**, 45 (2005).
[44] J. Akola and H. Häkkinen, Phys. Rev. B **74**, 165404 (2006).
[45] R. Varns and P. Strange, J. Phys.: Condens. Matter **20**, 225005 (2008).
[46] A. Marletta, A. A. Hidalgo, and R.A. Silva (to be published).